



Destructive impact of successive high magnitude earthquakes occurred in Türkiye's Kahramanmaraş on February 6, 2023

Aydin Demir¹ · Erkan Celebi¹ · Hakan Ozturk¹ · Zeki Ozcan¹ · Askin Ozocak¹ · Ertan Bol¹ · Sedat Sert¹ · F. Zehra Sahin¹ · Eylem Arslan¹ · Zeynep Dere Yaman¹ · Murat Utkucu² · Necati Mert¹

Received: 2 August 2023 / Accepted: 11 January 2024
© The Author(s) 2024

Abstract

Two successive earthquakes with moment magnitudes of $M_w = 7.7$ (focal depth=8.6 km) and $M_w = 7.6$ (focal depth=7 km) occurred approximately within 9 h on February 6, 2023, in Türkiye, respectively. The epicenters were the Pazarcık and Elbistan districts of Kahramanmaraş. Both earthquakes occurred in the East Anatolian Fault Zone, one of Türkiye's two major active fault systems. Between these two severe earthquakes, there was one more big aftershock with a moment magnitude of 6.6, the epicenter of which was in the Nurdağı District of Gaziantep. Then, on February 20, 2023, another aftershock earthquake with a magnitude of $M_w = 6.4$ occurred in Yayladağı district of Hatay. As a result of the earthquakes, severe damage occurred in several provinces and districts with a population of around 15 million, and more than 50,000 people have lost their lives. This study presents on-site geotechnical and structural investigations by a team of researchers after the Kahramanmaraş earthquakes. It summarizes the performance of the building environments as a result of on-site assessments, taking into account observed structural damage, local site conditions, and strong ground motion data. The possible causes of the observed damage are addressed in detail. These earthquakes once again revealed the common deficiencies of existing reinforced concrete structures in Türkiye, such as poor material quality, poor workmanship, unsuitability of reinforcement detailing, and inadequate earthquake-resistant construction techniques. Precast concrete and masonry structures in the region were also severely damaged during the earthquakes due to insufficient engineering service, poor materials, deficiencies during construction, etc.

Keywords Earthquake reconnaissance · Earthquake damage · Kahramanmaraş earthquakes · Reinforced concrete structures · Precast concrete structures · Masonry structures

1 Introduction

Türkiye and its surroundings, which are exposed to compressional tectonic processes under the influence of the Eurasian, Arabian, and African plates, are located on the highly seismically active Anatolian plate, where major earthquakes have occurred throughout history (McKenzie 1972; Şengör and Yılmaz 1981). The most crucial fault zones in the Anatolian region are The North Anatolian Fault Zone (NAFZ) and the East Anatolian Fault Zone (EAFZ), which show strike-slip characteristics. These fault zones cause the movement of the Anatolian plate to the west in a counterclockwise direction, and as a result of this activity, quite destructive earthquakes have occurred in Anatolia and its immediate surroundings (Barka and Kadinsky-Cade 1988; Duman and Emre 2013). Although the NAFZ, which is approximately 1500 km long, has a right-lateral strike feature, the EAFZ, which has a length of approximately 550 km, is left-lateral strike-slip (Fig. 1) (Şengör et al. 1985; Barka and Reilinger 1997).

From 1900 to the present, 20 earthquakes with a moment magnitude (M_w) greater than 7.0 have occurred in Türkiye. In addition, another 269 earthquakes with different magnitudes happened between 1900 and 2023, causing damage and casualties. The most significant ones are 1939 Erzincan ($M_s = 7.9$), 1944 Gerede ($M_s = 7.3$), 1999 Kocaeli ($M_w = 7.8$) and Düzce ($M_w = 7.5$), 2011 Van ($M_w = 7.2$), and 2023 Kahramanmaraş ($M_w = 7.7$ and $M_w = 7.6$) earthquakes (ITU 2023). Among them, the severest earthquakes in terms of casualties and heavy damage are the 1939 Erzincan, 1999 Gölcük-centered Kocaeli, and 2023 Kahramanmaraş earthquakes, respectively.

According to the records of the Disaster and Emergency Presidency of Türkiye (AFAD), on February 6, 2023, two earthquakes with magnitudes of $M_w = 7.7$ (focal depth=8.6 km) and $M_w = 7.6$ (focal depth=7 km) occurred at 04:17 (GMT+3) and approximately 9 h later at 13:24, respectively. The epicenters were Pazarcık and Elbistan districts of Kahramanmaraş. Both earthquakes occurred on the EAFZ, one of Türkiye's two major active fault systems. As a result of the earthquakes, damage experienced in the provinces and districts of Kahramanmaraş, Hatay, Gaziantep, Adıyaman, Malatya, Kilis, Adana, Diyarbakır, Osmaniye, Elazığ, and Şanlıurfa with a total population of more than 15 million people. These earthquakes have been recorded as the second and third-largest earthquakes in Türkiye. Between these two severe earthquakes, one more aftershock with a moment magnitude of 6.6 occurred at the epicenter of Nurdağı District of Gaziantep. That aftershock has been the largest recorded in the region. Afterward, another aftershock with a magnitude of $M_w = 6.4$ occurred in Yayladağı district of Hatay province on February 20, 2023, at 20:04 (GMT+3) (AFAD 2023).

The earthquakes in question caused great destruction in eleven provinces in total. These earthquakes are unprecedented disasters in recent history regarding intensity and area covered. As a result of the earthquakes, more than 50,000 people lost their lives, and more than half a million buildings were severely damaged. Communication and energy infrastructures were also heavily damaged, and significant financial losses have also occurred. As of March 6, 2023, damage assessment studies were carried out on 1,712,182 buildings. As a result, it has been determined that 35,355 buildings were destroyed, 17,491 buildings needed to be demolished urgently, 179,786 buildings were heavily damaged, 40,228 buildings were moderately damaged, and 431,421 buildings were slightly damaged. The damage distribution of structures in eleven provinces is presented in Table 1. The collapsed or severely damaged

Table 1 Damage distribution of damaged structures as of March 6, 2023 (PSBD 2023)

Province	Severely damaged or collapsed buildings	Moderately damaged buildings	Slightly damaged buildings
Adana	2,952	11,768	71,072
Adıyaman	56,256	18,715	72,729
Diyarbakır	8,602	11,209	113,223
Elazığ	10,156	15,22	31,151
Gaziantep	29,155	20,251	236,497
Kahramanmaraş	99,326	17,887	161,137
Malatya	71,519	12,801	107,765
Hatay	215,255	25,957	189,317
Kilis	2,514	1,303	27,969
Osmaniye	16,111	4,122	69,466
Şanlıurfa	6,163	6,041	199,401
Total	518,009	131,577	1,279,727

buildings also include historical and cultural structures, schools, administrative buildings, hospitals, and hotels, in addition to those used as residential buildings (PSBD 2023).

Because earthquakes, as profound natural disasters, threaten human life, infrastructure, and societal well-being, rapid and accurate reconnaissance following an earthquake event plays a vital role in assessing the extent of damage, identifying vulnerable areas, and informing emergency response efforts. Such reconnaissance endeavors provide invaluable insights into the complex dynamics of seismic events and contribute to the advancement of earthquake engineering and disaster management practices (Garini et al. 2017; Demir 2022; Sagbas et al. 2023). This study presents on-site geotechnical and structural investigations by researchers from the Civil Engineering and Geophysical Engineering Departments of Sakarya University after the Kahramanmaraş earthquakes. The observations have been performed in Kahramanmaraş, Gaziantep, Hatay, Adıyaman, and Malatya provinces, districts, and villages. The study summarizes the performance of the building environments as a result of on-site assessments, taking into account observed structural damage, local site conditions, and strong ground motion data provided by AFAD. The possible causes of the observed damage are addressed in detail. As demonstrated by numerous past earthquakes in Turkey, these recent seismic events have again exposed the prevailing shortcomings of existing reinforced concrete structures. These deficiencies include subpar material quality, inadequate construction practices, improper reinforcement detailing, and insufficient earthquake-resistant techniques. In conclusion, the study extensively examines the various types, characteristics, and underlying causes of building damage.

2 Geological evaluation (tectonic settings overview)

The EAFZ and NAFZ are continental transform faults and accommodate the westward motion of the Anatolian Plate caused by the northward motions of the African and Arabian plates with respect to the fixed Eurasian Plate (McKenzie 1972; Barka and Kadinsky-Cade 1988; McClusky et al. 2000; Reilinger et al. 2006). The EAFZ extends from Karlıova Triple Junction, where both transform faults join each other, to Antakya in the south, merging with

the Dead Sea Fault (Fig. 1) (Barka and Kadinsky-Cade 1988; Taymaz et al. 1991; Duman and Emre 2013).

A sequence of six large destructive earthquakes was generated by the EAFZ in the 19th century (Fig. 1). Adding the 1905 Malatya earthquake, only Pazarcık Segment of the EAFZ remained unruptured (Nalbant et al. 2002; Duman and Emre 2013). This section of the EAFZ is called the “Maraş Seismic Gap,” which was partly and lastly ruptured by the 1114 and 1513 earthquakes. The EAFZ was proposed to be relatively silent with three large earthquakes, namely the 1905 Malatya, 1971 Bingöl, and 1998 Adana earthquakes in the 20th century (Ambraseys 1989; Taymaz et al. 1991; Utkucu et al. 2018). The lesser earthquake activity period seems to be ceased with the recent occurrence of the devastating 2023 Kahramanmaraş earthquakes and the earlier occurrence of the 2003 Bingöl ($M_w = 6.4$), the 2010 Elazığ-Başyurt ($M_w = 6.0$) and the 2020 Sivrice-Doğanyol ($M_w = 6.7$) earthquakes in the first quarter of the 21st century (Tan et al. 2011; Utkucu et al. 2018; Xu et al. 2020). The EAFZ also caused considerably lower magnitude seismicity in the instrumental period (e.g., after 1900) (Bulut et al. 2012; Duman and Emre 2013).

The recent 2023 Pazarcık earthquake's ($M_w = 7.7$) rupture filled the Maraş Seismic Gap with no significant earthquake occurrence since 1513 (Fig. 1). Adding the stress load from the background extensive earthquake activity (Nalbant et al. 2002), the event of the 2023 Pazarcık earthquake was not a surprise. Nevertheless, it was a surprise that the 2023 Elbistan earthquake occurred along the Northern Strand of the EAFZ. The compiled hypocentral and source parameters of the earthquakes, given in Table 2, confirm that faulting is sinistral for both earthquakes and strikes NE-SW and E-W for the first and latter mainshocks, respectively. The earthquakes produced apparent surface ruptures of 270 km and 150 km long for the first and the second mainshocks, respectively (AFAD 2023; Karabacak et al. 2023).

The seismicity in Fig. 1 includes $M_w \geq 4.0$ earthquakes after 1970 (white circles), damaging historical earthquakes (pink-shaded ellipses), and $M_S \geq 6.2$ instrumental earthquakes (white and red stars). Large arrows indicate the direction of relative plate motions (see Fig. 1). The seismicity is taken from Kandilli Observatory and Earthquake Research Institute (KOERI) and Ambraseys (1989). Surface ruptures of the 2023 Pazarcık and Elbistan earthquakes are demonstrated with thick red and blue lines, respectively. Moreover, in Fig. 1, NS: Northern Strand of the EAFZ, BTZ: Bitlis Thrust Zone, KTJ: Karliova Triple Junction, DFZ: The Dead Sea Fault Zone, AS: Amanos Segment, PS: Pazarcık Segment,

Table 2 The hypocentral and source parameters of the February 6, 2023, earthquake sequence

Date	Origin time (GMT+3)	Lat.	Long.	Depth	M_w (GCMT)	Strike	Dip	Rake	Refer- ence
<i>February 6, 2023, Mainshock 1, 01:17 ($M_w = 7.7$)</i>									
06.02.2023	01:17:35	37.1736	37.032	17.9	7.8	228	89	-1	USGS
06.02.2023	01:17:31	37.1123	37.1195	5	7.7	222	64	-27	KOERI
06.02.2023	01:17:32	37.288	37.043	8.6	7.7				AFAD
06.02.2013	01:18:10	37.56	37.47	14.9	7.8	54	70	11	GCMT
<i>February 6, 2023, Mainshock 2 10:24 ($M_w = 7.6$)</i>									
06.02.2023	10:24:49	38.024	37.203	10.0	7.5	277	78	4	USGS
06.03.2023	10:24:46	38.0717	37.2063	5	7.5				KOERI
06.02.2023	10:24:47	38.089	37.239	7	7.6				AFAD
06.02.2023	10:24:59	38.11	37.22	12	7.7	261	42	-8	GCMT

GCMT: Global Centroid Moment Tensor; USGS: United States Geological Surveys

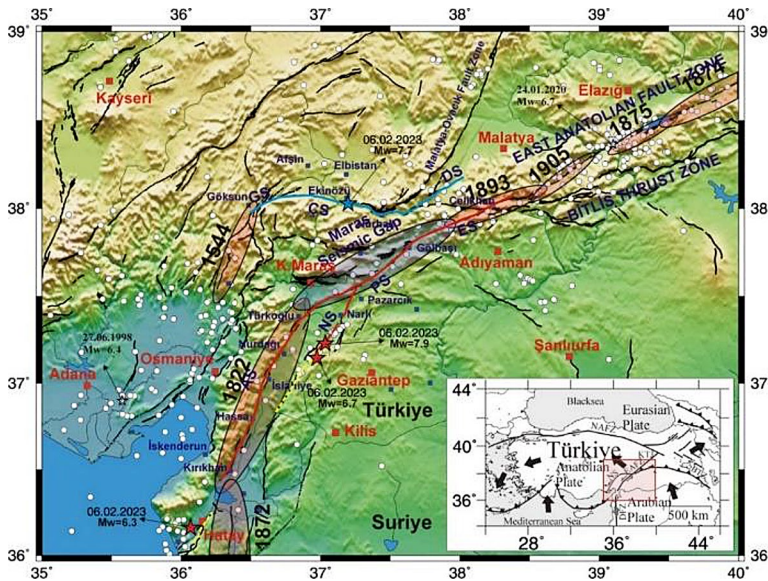


Fig. 1 The general tectonic configuration of Türkiye (inset) and the seismotectonic features of the EAFZ

ES: Erkenek Segment; NS: Nurlu Segment, GS: Gökşun Segment, CS: Çardak Segment and DS: Doğanşehir Segment (Compiled from Barka and Kadinsky-Cade (1988), Ambraseys (1989), McClusky et al. (2000), Emre et al. (2013), Duman and Emre (2013).

3 Strong ground motion and response Spectra

The earthquakes were recorded by many seismic stations existing in AFAD’s Turkish national strong motion network. Some of the ground motion stations located in the earthquake-affected area and recorded peak ground acceleration (PGA) values as of November 2, 2023, are reported in Tables 3 and 4 for Pazarcık Earthquake ($M_w = 7.7$) and Elbistan Earthquake ($M_w = 7.6$), respectively. The distance of the stations to the epicenter locations (R_{epi}), the station’s soil shear wave velocity ($V_{s,30}$), and the corresponding soil classes defined in the Turkish Building Earthquake Code 2018 (TBEC 2018) are given in those tables as well. The maximum PGAs were recorded at station 4614 for the Pazarcık Earthquake ($M_w = 7.7$) as 2.056 g in East-West (E-W), 2.079 g in North-South (N-S), and 1.613 g in Up-Down (U-D) directions. They were 0.533 g in the E-W direction and 0.648 g in the N-S direction for the Elbistan Earthquake ($M_w = 7.6$) recorded at station 4612, and 0.622 g in the U-D direction at station 4631. Some recorded acceleration, velocity, and displacement time history plots of the stations with maximum PGAs are depicted in Figs. A1 and A2 in the Appendix. Moreover, the calculated Arias Intensities are plotted with accelerations in the same figures. The calculated acceleration response spectra are also illustrated in Figs. 2 and 3 for the same stations.

Upon the horizontal and vertical elastic design spectra are investigated, it is observed that the elastic design spectrum, created for an earthquake risk having a return period of 475 years (corresponding to earthquake level DD-2 in TBEC 2018) was exceeded in the

Table 3 Ground motion stations and recorded PGAs for Pazarcık Earthquake ($M_w = 7.7$) (TADAS 2023)

Station code	Province	District	Latitude	Longitude	R_{epi} (km)	$V_{s,30}$ (m/s)	Soil Class	PGA (g)		
								N-S	E-W	U-D
0131	Adana	Saimbeyli	37.8566	36.1153	103	N/A	N/A	0.159	0.163	0.050
0201	Adıyaman	Merkez	37.7612	38.2674	120	391	ZC	0.483	0.897	0.325
2104	Diyarbakır	Ergani	38.2644	39.7590	262	N/A	N/A	0.074	0.119	0.082
2310	Elazığ	Baskil	38.5726	38.8245	212	N/A	N/A	0.062	0.052	0.050
2718	Gaziantep	İslahiye	37.0077	36.6266	48	N/A	N/A	0.667	0.643	0.604
2712	Gaziantep	Nurdağı	37.1840	36.7328	30	N/A	N/A	0.566	0.604	0.320
3129	Hatay	Defne	36.1911	36.1343	146	447	ZC	1.378	1.222	0.731
3126	Hatay	Antakya	36.2202	36.1375	144	350	ZD	1.201	1.019	0.939
4614	Kahramanmaraş	Pazarcık	37.4851	37.2977	31	541	ZC	2.056	2.079	1.613
4616	Kahramanmaraş	Türkoglu	37.3754	36.8383	21	390	ZC	0.622	0.437	0.395
7901	Kilis	Merkez	36.7088	37.1123	65	463	ZC	0.054	0.017	0.051
4414	Malatya	Kale	38.4069	38.7541	195	N/A	N/A	0.109	0.167	0.052
8002	Osmaniye	Bahçe	37.19156	36.5619	44	430	ZC	0.248	0.207	0.343
6304	Şanlıurfa	Bozova	37.36509	38.5131	130	376	ZC	0.215	0.243	0.091

Table 4 Ground motion stations and recorded PGAs for Elbistan Earthquake ($M_w = 7.6$) (TADAS 2023)

Station code	Province	District	Latitude	Longitude	R_{epi} (km)	$V_{s,30}$ (m/s)	Soil class	PGA (g)		
								N-S	E-W	U-D
0131	Adana	Saimbeyli	37.8566	36.1153	102	N/A	N/A	0.410	0.338	0.087
0213	Adıyaman	Tut	37.79667	37.9295	69	N/A	N/A	0.124	0.129	0.073
2107	Diyarbakır	Çermik	38.14594	39.4837	196	N/A	N/A	0.029	0.049	0.019
2308	Elazığ	Sivrice	38.45063	39.3102	185	450	ZC	0.071	0.049	0.034
2703	Gaziantep	Şahinbey	37.058	37.3500	115	758	ZC	0.095	0.065	0.028
3144	Hatay	Hassa	36.75691	36.4857	162	485	ZC	0.060	0.080	0.028
4612	Kahramanmaraş	Göksun	38.02395	36.4818	67	246	ZD	0.648	0.533	0.504
4631	Kahramanmaraş	Nurhak	37.96633	37.4276	21	543	ZC	0.344	0.396	0.622
7901	Kilis	Merkez	36.7088	37.1123	154	463	ZC	0.052	0.051	0.023
4406	Malatya	Akçadağ	38.3439	37.9738	70	815	ZB	0.476	0.417	0.325
8003	Osmaniye	Merkez	37.08417	36.2693	141	350	ZD	0.050	0.068	0.030
6306	Şanlıurfa	Akçakale	36.7277	38.9470	214	N/A	N/A	0.037	0.028	0.014

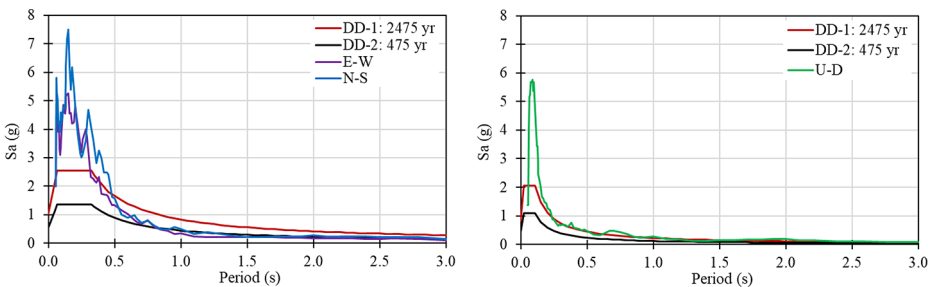


Fig. 2 Pazarcık Earthquake ($M_w = 7.7$), Station 4614 (Kahramanmaraş/Pazarcık), Response Spectra ($\xi = 5\%$, $V_{s,30} = 541$ m/s, Soil class: ZC)

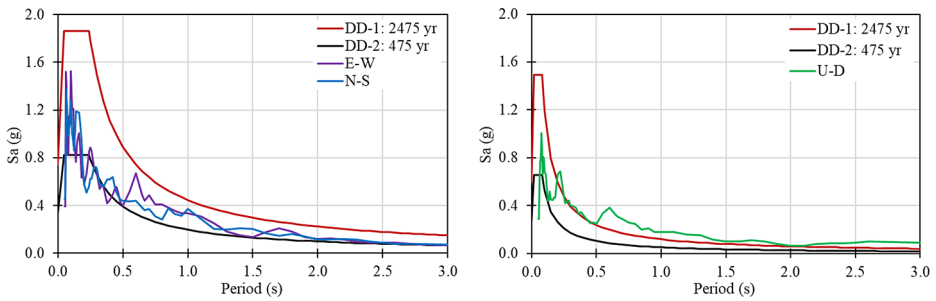


Fig. 3 Elbistan Earthquake ($M_w = 7.6$), Station 4406 (Malatya/Akçadağ), Response Spectra ($\xi = 5\%$, $V_{s,30} = 815$ m/s, Soil class: ZB)

locations of Karamanmaras, Hatay, Gaziantep, and Adıyaman during the Pazarcık Earthquake ($M_w = 7.7$). However, the elastic design spectrum created for an earthquake risk having a return period of 2475 years (corresponding to earthquake level DD-1 in TBEC 2018) was only exceeded in Karamanmaras and Hatay provinces. Moreover, during the Elbistan Earthquake ($M_w = 7.6$), while the design spectrum created for DD-2 was exceeded only in Malatya and Karamanmaraş, the design spectrum of DD-1 earthquake level was not exceeded in the region except at station 4612 in Elbistan for the periods higher than 1.2 s. The design spectra have not been exceeded in other places in the area.

Additionally, it is determined that the earthquakes mainly affected the short-period buildings having a fundamental period of lower than 1.0 s and corresponding to low and mid-story structures. Therefore, the damage increased in the region because it generally has low and mid-story building stock. Nevertheless, the buildings with large periods seemed affected only at station 4612. Moreover, the buildings with large overhangs were also severely damaged in the region because the vertical components of the recordings were very high and exceeded the design spectra.

4 Geotechnical overview

The recent 2023 Kahramanmaraş earthquakes have caused many geotechnical problems in addition to severe damage to the structures in the region. In the field surveys carried out after the earthquakes, it has been observed that significant damage was experienced in the region due to geotechnical reasons, especially in İskenderun district of Hatay province and Gölbaşı district of Adıyaman province. Lateral spreading events as well as ground liquefaction were also encountered in the observations. Apart from those, many mass movements triggered by earthquakes have been reported. Hatay's İskenderun district and Adıyaman's Gölbaşı district are regions where liquefaction and lateral spread are commonly observed. In this section, on-site geotechnical observations after the earthquakes are presented.

Soil liquefaction is defined as a significant loss of strength and stiffness due to the development of excess pore water pressures resulting in zero effective stress in the soil during a seismic event (Cetin and Ilgac 2023). The soil liquefaction phenomena were predominantly observed in the İskenderun district of Hatay, affecting both existing structures and open areas. Some examples of observed liquefaction-induced sand ejecta surrounding the build-



Fig. 4 Uniform settlement of a building (left) and sand ejecta around a structure (right) in Iskenderun coastal region of Hatay



Fig. 5 Sand cones and crater geometries along the coastline (left) and some of the damages on road structures (right) in Iskenderun district of Hatay

ings in Iskenderun's coastal part are presented in Fig. 4. The field investigations here have shown that the liquefied sand reached out of the surface, especially from the corners and edges of buildings. The structures have made a uniform settlement between 30 and 50 cm but have maintained their functions.

Moreover, towards the coastline, commonly, liquefaction and sand cones phenomena in open areas were observed. An example of the sand cones and ejecta can be seen in Fig. 5. Considering the number and volume of the cones, it has been determined that the liquefaction has spread over a wide area here. As a result of that widespread liquefaction occurred in this region; a large amount of water reached out of the ground surface with the liquefied sand. This also caused floods on the coastline, especially along Atatürk Boulevard. Excessive deformations in road structures due to settlements and sand ejecta also became a striking point of the observations (see Fig. 5).

Soil liquefaction phenomena were also observed in Antakya (Demirköprü), Arsuz, Kırıkhan and Dört Yol districts of Hatay. Lateral spreading, observed on the coastal part of Dört Yol district,



Fig. 6 Liquefaction-induced failures observed in Dörtyol district of Hatay



Fig. 7 Landslide damage observed in Antakya (left) and in Altınözü (right) districts of Hatay

is given in Fig. 6a. Sand ejecta were observed in the free-field here (Fig. 6b) as a result of lateral spreading caused by liquefaction. As a result of this spread, a failure surface of approximately 900 m length was formed. It was determined that the buildings in the western part of Dörtyol district were exposed to about 80 cm vertical settlements in addition to the lateral deformations. Some apparent examples of these deformations can be seen in Fig. 6c, d.

Apart from liquefaction, geotechnical damages were also detected in Antakya city center. The first of these was the small-scale slides in the Asi River, which passes through the middle of the city center. Another damage is the large-scale landslide that occurred in Altınözü, approximately 200 m long and 400 m wide. It has been observed that weak sedimentary rocks dominate at the base of the landslide area. The mentioned damages are shown in Fig. 7.

Liquefaction-induced geotechnical damage was also observed in Gölbaşı district of Adiyaman, consisting of quaternary alluvial plains. The region generally has two young units: alluvium and marsh sediments. Alluvium consists of greenish-light brown, brown-colored gravel, sand, and clay layers and occasionally contains silt bands. Gravel and sand units are also variably stratified in lateral and vertical directions. The swamp sediments are located around Gölbaşı lake, west of Gölbaşı city center. They generally consist of black, dark brownish, dark grayish colored very fine silt and mud-sized sediments and contain abundant organic matter. Since the groundwater level in these areas is at or close to the surface, it mixes with clayey and silty levels, giving the ground a swamp-sludge feature (Akıl et al. 2008).

Lastly, during the Kahramanmaraş earthquakes, widespread soil problems were observed in the Gölbaşı area. Many buildings have faced issues such as excessive settlement, tilting and toppling over, etc. These problems are thought to arise from the poor earthquake performance of young alluvial soils with a high groundwater level. Additionally, the presence of sand ejecta in the free-field was also determined, as presented in Fig. 8. A building, near the close vicinity to this sand ejecta, was toppled over along the short side of the foundation. This indicates that liquefaction phenomena have caused many soil problems in Gölbaşı. The low depth of the foundation and the high length-to-width ratio of the building were also determined to facilitate the toppling. Consequently, it has been deduced that similar to past earthquakes, the necessity of considering the soil characteristics in the infrastructure design and construction has emerged again after the recent Kahramanmaraş earthquakes to ensure the safety of the infrastructures to be built in earthquake zones.

5 Seismic response of cast-in-place reinforced concrete structures

Most reinforced concrete (RC) structures have been built as cast-in-place in the region, including low and mid-story residential apartments and office buildings. Their story numbers range from 1 to 15. Some buildings designed for the residential occupancy class have commercial spaces on their ground floors with a higher story height than the upper stories. Some of them have mezzanine stories as well. The load-bearing system of the majority of them was constituted with moment-resisting frames. Some of them also include shear walls. Most of the RC buildings in the region were constructed before 2000 without having sufficient engineering services. Therefore, many of them were severely damaged and collapsed during the earthquakes. The leading causes observed in severely damaged or collapsed buildings are poor material quality, soft story effect, strong beam-weak column behavior, large and heavy overhangs, insufficient beam-column joints, unconfined infill, gable walls, etc. Some of them are explained in detail in this section.

The residential buildings have been generally built within the development and update process of the Turkish Earthquake Code in 1967, 1975, 1998, and 2018. The 1998 code is a specification in which the concept of ductility, column-beam connection design, and strong column-weak beam design are discussed for the first time in Türkiye regarding earthquake-

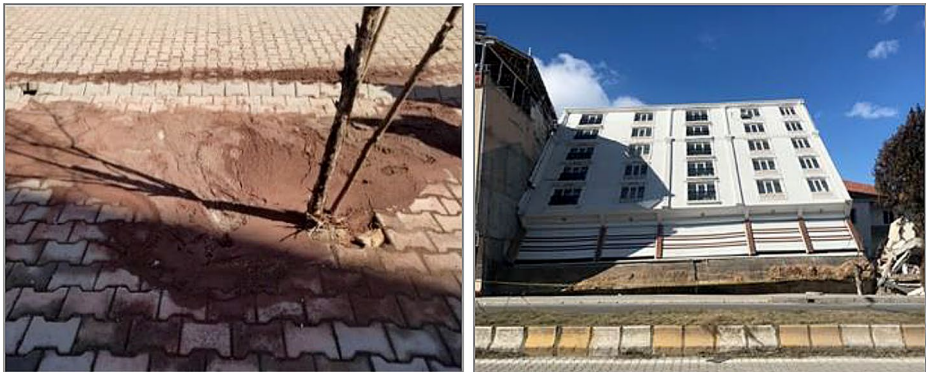


Fig. 8 Sand ejecta (left) and an overturned building (right) in Gölbaşı district of Adıyaman

resistant structures. As a result of the site investigations within the scope of this regulation, it has been observed that the columns have weak sections compared to the beams and that designs are unsuitable for the strong column-weak beam principle in most residential buildings throughout the region. That caused the formation of plastic hinges at the upper and lower ends of the columns.

The general building stock has been observed to consist of frame systems with low aspect ratios. While this reduces the seismic force on the structure, it also causes structures to behave flexibly and have larger periods. In fact, in the field surveys conducted throughout the region, column joints at the ground floor foundation or basement walls have caused hinges even in new buildings. Due to the large displacements, it has been observed that concrete was crushed, and reinforcement was buckled or ruptured in the areas where hinges occurred. In buildings with rigid ground floors, hinges have been observed at the endpoints of the ground-floor columns (Fig. 9a). Flexure and shear cracks caused by seismic forces have also been observed in beams (Fig. 9b). Damage has been observed in beams due to torsion and stair landings due to the torsion effect (Fig. 9c).

5.1 Poor concrete quality and wrong placement of concrete

The quality of concrete is one of the most essential parameters in structural performance. Therefore, the minimum concrete quality used in the buildings has been defined as 18 MPa in the 1975 code, 20 MPa in the 1998 and 2007 codes, and 25 MPa in the Turkish Buildings Earthquake Code 2018. However, despite the presence of limit values for concrete quality in the regulations, an examination of concrete samples obtained from structures damaged during earthquakes has revealed that the concrete quality is far below the limits defined in the specifications. The reasons for this include the lack of appropriate mixing ratio, absence of suitable aggregate gradation (large-sized and smooth-surfaced aggregate), lack of vibration, segregation, and presence of foreign materials in the concrete (such as plastic, paper, wood, etc.). Field observations have identified certain drawbacks directly affecting concrete quality, such as inappropriate aggregate sizes, segregation, and the presence of foreign materials.

Most buildings constructed before 2000 were built using man-made concrete mixed and manufactured by human labor. Therefore, they have common mistakes such as wrong concrete mix (wrong water, cement, and aggregate ratio), low cement ratio, the existence of organic and inorganic materials in the mix, very small or massive aggregate, wrong place-

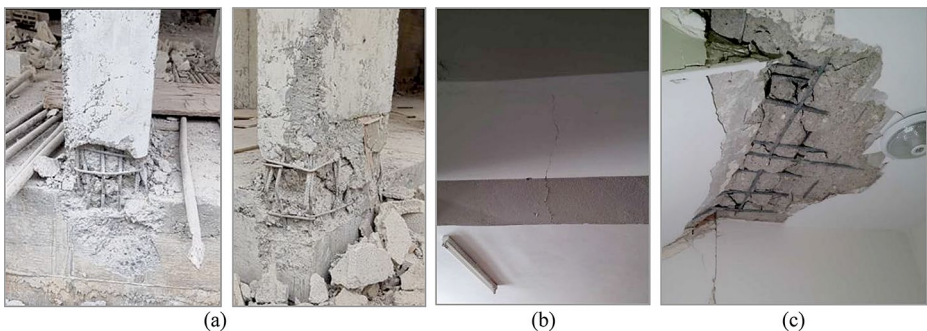


Fig. 9 Examples of plastic hinges at the bottom of columns (a), flexure cracks in beams (b), and damage in stair landings (c)

ment of concrete (heavy segregation), etc. some examples of poor concrete quality and segregation are depicted in Fig. 10.

5.2 Poor reinforcing steel quality, corrosion, and improper placement of reinforcement

The bonding between the concrete and the reinforcement must be established for reinforced concrete structural elements to exhibit the expected ductile behavior. The bonding between concrete and reinforcement is a crucial parameter that enables these two materials to work together. Ribbed reinforcements are produced by creating notches on the surface of the reinforcement to increase bonding. However, while the use of ribbed reinforcement was not mandatory in the past, it became compulsory in 1998 in the Turkish Earthquake Code. Until then, smooth reinforcement and poor-quality concrete have resulted in reinforced concrete structures with weak bonds (Olabi et al. 2022). Some of these structures have also been found to have corrosion on reinforcement. Due to the corrosion-induced section loss in the reinforcement, bonding weakens, and the load-bearing capacity of RC members decreases (Less et al. 2023). Additionally, non-compliant practices with regulatory details have been observed in the placement of transverse reinforcements (stirrups) in structural elements, such as inadequate, irregular, hookless, and excessive spacing. As in previous earthquakes, inadequate, poor-quality, smooth reinforcement, reinforcement corrosion, and poor workmanship in reinforcement and concrete have caused significant damage to reinforced concrete structures during the 2023 Kahramanmaraş earthquakes.

Additionally, it has been observed that plain reinforcing steel was generally used in buildings constructed before 2000. The reinforcement steel also had significant corrosion due to insufficient concrete cover (Fig. 11a). Concrete segregation has also been detected in these buildings (Fig. 11b). In many buildings, stirrups were bent wrongly at 90-degree instead of 135-degree, as prescribed in the TBEC 2018 (Fig. 11c). In many buildings in the region, it was observed that the protruding reinforcement bars of columns and walls from the foundation did not comply with the overlapping length requirement specified in the regulations. In these areas, due to the lack of proper spacing between reinforcement bars and the bending



Fig. 10 Examples of poor concrete quality (a) and wrong placement of concrete (segregation) (b)

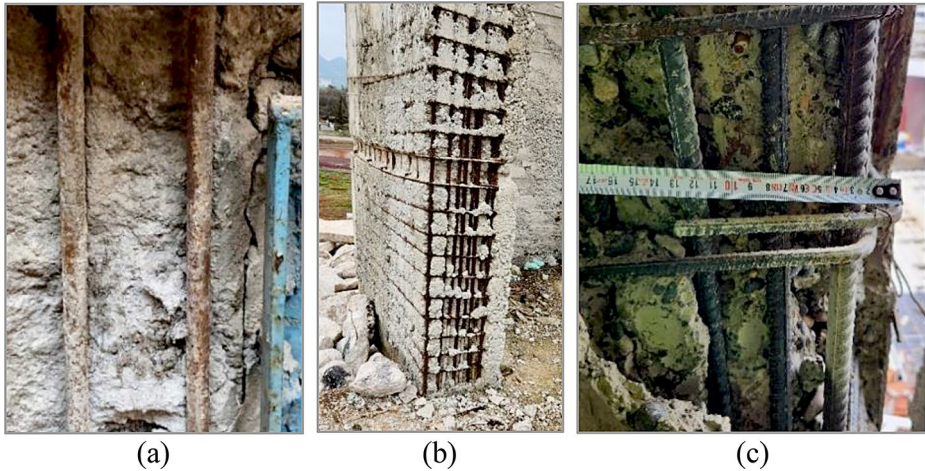


Fig. 11 Unribbed smooth reinforcement and heavy corrosion (a), insufficient concrete cover and heavy segregation (b), and wrongly bent stirrups (90-degree bent) (c)

of reinforcing bars at 90-degree angles, plastic hinges have formed at the bottom of the columns, causing concrete cracking and reinforcement deformation.

5.3 Soft story effects in ribbed slab constructions

The heavily damaged and collapsed reinforced concrete buildings, which were generally constructed after 2000 years in the densely populated settlements such as Nurdağı, İslahiye, Pazarcık, Türkoğlu, Kırıkhan, and Antakya, are examined closely in the post-earthquake region. Notably, they have similar architectural features and were arranged with the same type of load-bearing system, especially for the floor members. As can be seen from Figs. 12 and 13, the first two floors of such multi-story buildings have been designed for commercial workplace purposes, and the floors above them are used as residential areas with large and heavy overhangs. It has been observed in the field that these types of apartment buildings with similar engineering and architectural design errors failed against seismic forces.

Moreover, examining the building stocks in the earthquake-hit regions, one-way ribbed slabs have generally been widely used in the load-bearing systems of five- to eight-story buildings. It is remarkable to note that the vertical structural elements carrying these types of floor slabs have not been supported by shear walls as clearly specified in the TBEC (2018). Many residential structures having ribbed slab systems (using lightweight briquette blocks or styrofoam between floor joists) were severely damaged due to inadequate shear resistance because they could not exhibit rigid diaphragm behavior. Apparently, the ribbed slab applications in RC structures that are incompatible with the restrictions imposed on such beamless plates in the earthquake codes have caused heavy damage or destruction triggered by the soft story effect. The seismic energy transmitted to the structure was not consumed as required at the beam ends in line with the strong column-weak beam principle. On the contrary, the energy consumption points resulted in the formation of plastic hinges at the whole column ends of the ground floor in the immediate initial vibrations of the earthquake ground motion, making the structure unable to bear the seismic shear forces. Ultimately,

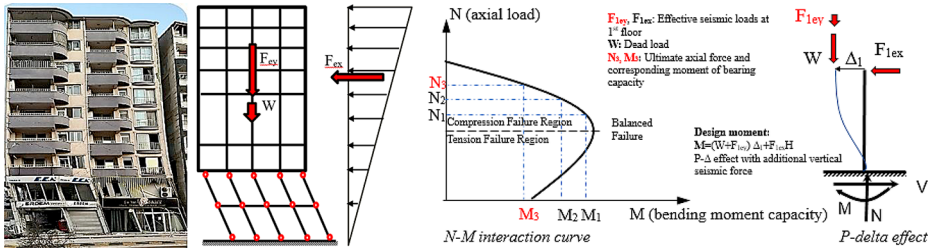


Fig. 12 Collapse mechanism due to soft story effect: P-delta effects with additional vertical inertial forces



(a) Building 1, before (left) and after (right) earthquakes (b) Building 2, before (left) and after (right) earthquakes

Fig. 13 Examples of typical buildings in the earthquake-hit region and heavy structural damages due to engineering and architectural design errors

it can be clearly seen in Fig. 12 that the upper residential floors of such buildings become unusable by making a rigid movement compared to the lower-story floors without shaking during the vibration period.

It should also be noted that the vertical accelerations generated by the 2023 Kahramanmaraş earthquakes were as effective as the horizontal acceleration components. Therefore, especially the buildings designed with ribbed floor slabs were subjected to significant seismic forces. In this case, ribbed slab construction leads to additional axial loads on vertical structural members as they cannot show sufficient resistance against high vertical accelerations like conventional two-way beam-supported slabs. While the moments of bearing capacity at the ground floor columns decreased drastically with the increase of the axial load, the second-moment effects emerged because of the earthquake’s excessive displacement demand on these floors, and the design moment on these load-bearing elements increased significantly (Fig. 12). As shown in Fig. 13, the stability of individual column members on the ground floor was influenced adversely by the increased number of plastic hinges triggering the collapse mechanism of soft story action due to the demand of undesired large story drift depending on the additional vertical inertia forces.

The lateral load-bearing systems with a high ductility level proposed for ribbed floor slabs in the earthquake-affected areas have generally not been designed per the Turkish Earthquake Codes involving special design provisions to avoid soft story effects. As a result of modeling the floor as a rigid diaphragm in computer-aided structural analysis, it is determined that the earthquake loads cannot be fully transferred to the vertical elements properly. Turkish Building Earthquake Code considers the load-bearing systems of buildings with ribbed floor slabs not supported by shear walls as having limited ductility. However, it also allows the construction of

such buildings in regions with low seismicity. In other words, it doubles seismic loads for the structural design of ribbed floor constructions compared to two-way slab systems.

5.4 Strong beam and weak column behavior

During earthquakes, column-beam joint regions are subjected to significant forces. If these forces exceed the strength of the column and beam, plastic hinges are formed in these regions. In order to prevent sudden and brittle failure, it is desired to have these plastic hinges form at the ends of the beams rather than at the ends of the columns. That ensures the principle of the strong column and weak beam behavior, as defined in the seismic design codes. Furthermore, to ensure sufficient rigidity in these regions, transverse reinforcement along the confinement zone should be densified according to the criteria specified in the specifications. However, field investigations have revealed that the practices mentioned earlier were not adequately implemented, significantly damaging the structures.

Additionally, the 1998 Turkish Earthquake Code is the first in Türkiye to address the concept of ductility for designing structures that will not collapse in earthquakes, as well as the design of column-beam joint regions and strong column-weak beam design. As a result of field surveys conducted under this regulation, it has been observed that in buildings constructed before 1998, columns have weaker cross-sections compared to beams. Most residential buildings in the region have not been designed to comply with the strong column-weak beam principle. Therefore, those buildings were severely damaged or collapsed during the Kahramanmaraş earthquakes. Lastly, the insufficient resistance of columns to beams has led to the formation of shear cracks and hinges at the top and bottom ends of the columns (Fig. 14).



Fig. 14 Examples of a strong beam weak column design and damage on columns

5.5 Large and heavy overhangs

It is prescribed in many earthquake design codes that external eccentricities that may occur in terms of mass, stiffness, and strength can be prevented by arranging a symmetrical structural system. As a result, a predictable seismic behavior can be achieved. When the damaged and collapsed buildings in the region were observed, it was determined that many buildings specifically located on main streets had extensive overhangs extending to 1.5 m. Moreover, the columns carrying those overhangs were not connected with the beams, and that caused the formation of an insufficient tied framing system. Therefore, the columns could not work together or provide proper load transfer (Fig. 15). Moreover, in earthquake-resistant building design, placing shear walls that can withstand a significant portion of the earthquake forces is important. In the region, even if shear walls were included in the buildings, it was observed that they were not symmetrically placed in structures. The resulting irregularity in torsion and the additional moment effects caused by the heavy overhangs resulted in the formation of plastic hinges at the end regions of all columns in the outer axis (Fig. 16a).

Additionally, one of the most essential structural problems observed in the areas affected by earthquakes is that existing buildings have been completed by the addition of new floors on the structures over the years without having any engineering services. During the construction of these additional floors, the load-bearing system of the existing floor, vertical element continuity in the new floors, cold joints between floors, construction techniques, and material differences were not considered. For example, the building in Fig. 16b was initially built as a single-story masonry ground floor. Over the years, a three-story RC structure was added, and finally, it was completed with a steel frame roof floor. While the original ground floor remained standing, the additional stories built on top collapsed during the earthquakes.

Lastly, many seismic codes never allow the placement of columns on the top or end of cantilever beams or on the gussets formed on the lower columns of any building floor. However, during the field surveys, plastic hinge occurrences have been observed in some buildings due to reinforcement bending and concrete pouring at the bottom of columns as a result of that practice (Fig. 17).

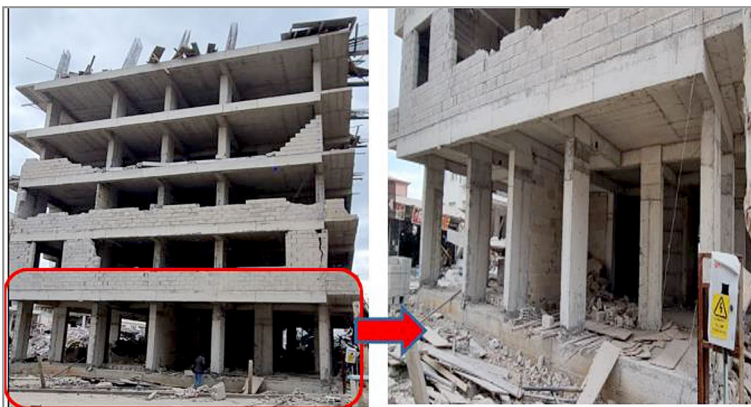


Fig. 15 Examples of large and heavy overhangs on RC buildings in the earthquake-hit region



Fig. 16 Examples of column damage due to large overhangs (a) and a building collapse due to additional floors (b)

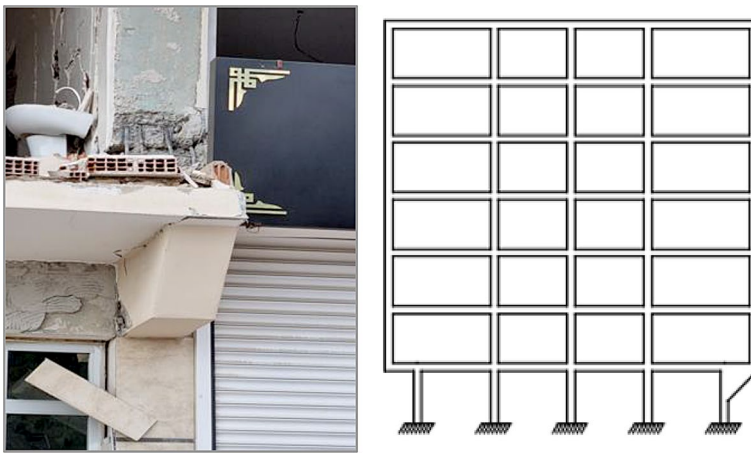


Fig. 17 An example of a column connecting on the end of cantilever beams (the right drawing from TBEC 2018)

6 Seismic response of precast concrete structures

Prefabricated structures built with precast reinforced concrete elements are used as production areas in industry. The components of such construction systems are produced in a factory environment in a controlled manner. Faster and controlled assembly of structural members in the field saves time and cost. Structural elements produced by this method are ahead of traditional construction techniques with their strength and dimensional stability. The production is based mainly on agriculture and animal husbandry, textile, metal and steel industry, paper industry, food production, and agricultural machinery production in the earthquake-hit region are made in such structures.

After the 2023 Kahramanmaraş earthquakes, a field investigation was conducted on the precast structures in and around Kahramanmaraş province, and the damage patterns were observed on those structures. The most common type of damage was the falling of the horizontal beams resting on the column corbels by disconnecting their joints. Similarly, damage to the ends of roof



Fig. 18 Examples of insufficient fastening of roof purlins to beams (a), and damage in joint regions (b)



Fig. 19 Floor damage due to poor connection detailing (left) and a precast concrete structure with weak columns and heavy roof beams (right)

purlins that were not adequately connected to the beams and falling of them to the ground was common (Fig. 18). The damage was generally caused by the inability of the structural elements to respond to the seismic displacement and rotation demands in joint regions, the weakness of the members in the joints, and pin connections that are not filled with cement mortar. Due to the lack of connection details, the precast floor elements sitting on the beams also separated from the connection points, disrupting the integrity of the building and could not show the diaphragm behavior supposed to be provided at floor levels (Fig. 18).

The architectural and structural system plans, which were arranged incorrectly, revealed the effects of torsion and caused the beams to be separated from the columns. For example, a 5-meter-high mezzanine floor was built in a part of a reinforced concrete precast building with a floor height of 10 m (see Fig. 19). In these two regions, the damage occurred due to the simultaneous rigid and flexible behavior that differs depending on the column lengths and the mezzanine diaphragm. Moreover, severe damage and collapses were widely observed in prefabricated structures with weak columns and heavy roof beams that could not provide horizontal stability (Fig. 19).

Additionally, infill wall damage in prefabricated buildings was also widespread. Low-strength, hollow briquettes, commonly called “bims” have been widely used in the structures located in the region. Due to low horizontal reinforced concrete beams providing stability in large-span walls and exceeding the maximum unsupported wall length, the out-of-plane movement occurred in the walls during the Kahramanmaraş earthquakes (Fig. 20). Moreover, the panels coming out of the slots supported on the columns or out-of-plane movement were one of the common and typical damages seen in the precast wall panels (Fig. 20).



Fig. 20 Examples of large-span walls exceeding the maximum unsupported wall length on the walls (left) and out-of-plane tipping damage on the precast wall panels (right)

Failure to perform the necessary precision quality to the joints during the production and assembly stages, filling the pins with low-strength cement mortar or not filling them at all, and insufficient or no use of nuts, washers, and welds caused significant damage on precast wall panels. Lastly, bending cracks at the lower end of the columns, separation of the shell concrete, buckling of the reinforcements, and damage up to the rupture of the reinforcement were also observed in the column-foundation nodes.

7 Seismic response of masonry structures

Historical monumental structures are the most valuable treasures that reflect the history of societies and nations and reveal their culture and civilization. Such structures are carefully preserved worldwide, as they show the levels and lifestyles of communities in culture and art, which connects societies' past to the future. The masonry construction technique is used all over the world for the construction of low and medium-rise buildings. Wood, adobe, brick, and stone are the oldest known building materials. These materials are still used today because of their cost-effectiveness, durability, local availability, and sound-insulating properties. Earthquake codes have been updated many times for the design and construction of such structures (Günaydin et al. 2021).

The data obtained from field surveys after the Kahramanmaraş earthquakes showed a significant fragility in the masonry building stock constructed using traditional methods and materials. Most of the buildings in the region have been built in the form of arched, vaulted, and domed structures with baked clay bricks, rubble stone, or cut stone masonry. Most buildings are unreinforced masonry structures characterized by rubble stone walls with two smooth surfaces connected. In some buildings, the diaphragms between the floors have been constructed with wood, steel, and brick materials using masonry. In addition to residences, public buildings, and factories in the region, Kahramanmaraş earthquakes also affected historical structures. They caused significant damage and collapse, specifically in Hatay, Adiyaman, Kahramanmaraş, and Gaziantep provinces. 65% of historical buildings in the region were destroyed or severely damaged. Macro seismic scale earthquake damages of magnitude IX-XI occurred in Antakya and Kahramanmaraş (KOERI, 2023). Excessive



Fig. 21 Habibi Neccar Mosque, Antakya, Hatay, before (left) and after (right) the Kahramanmaraş earthquakes



Fig. 22 Sarimiye Mosque, Antakya, Hatay, before (a) and after (b) the Kahramanmaraş earthquakes

ground motion demand in peak ground acceleration further increased the damage to structures damaged by previous shocks.

More than half of the buildings collapsed in the historical city center of Hatay. Among them, Habib-i Neccar Mosque, Sarimiye Mosque, Historical Saints Peter and Paul Church, Greek Orthodox Church, and Iskenderun Italian Latin Catholic Church are essential structures of our historical architectural heritage that were partially damaged or collapsed in the historical city center of Hatay. Those structures' pre- and post-earthquake situations are depicted throughout Figs. 21, 22, 23 and 24, respectively.

Moreover, the investigated historical buildings in Gaziantep, built mainly between the 17th century and the end of the 19th century, performed better seismic response due to being far from the fault line. Restored historical building examples showing good performance in the historical center of Gaziantep province were examined. Since these structures are relatively far from the fault line, the structures were exited with accelerations smaller than the design earthquake level of TBEC 2018. In the historical buildings inspected in Gaziantep province, slip cracks in the main walls, openings in the joints, and local separations in the outer layers of the walls were observed (see Fig. 25). There was damage to the joints of arches and vaults, and out-of-plane movements were detected at the wall-vault joints (Fig. 26). Opening at the joints, vertical cracks, and overturning on the pedestals were observed in the mosque's minarets (Fig. 27).



Fig. 23 The Historical Church of Saints Peter and Paul, Antakya, Hatay, before (left) and after (right) the Kahramanmaraş earthquakes



Fig. 24 Antakya Greek Orthodox Church (left) and Iskenderun Italian Latin Catholic Church (right) after the Kahramanmaraş earthquakes

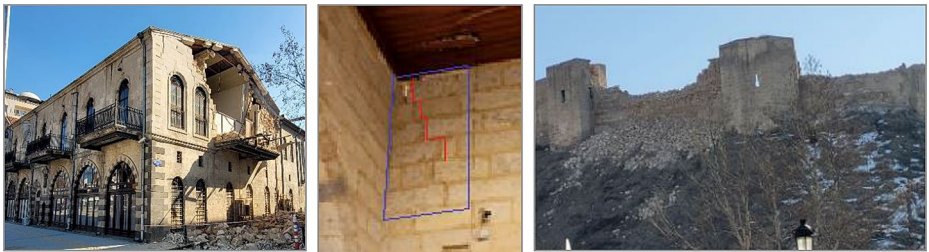


Fig. 25 Examples of damage to the structural main walls

Many factors have contributed to the collapse response of masonry structures during the 2023 Kahramanmaraş earthquakes. One of the most important factors is the characteristics and direction of the earthquake (directivity effect). This effect is more complex for historical buildings having different building elements with varying geometries. Establishing effective connections between horizontal slabs and vertical load-bearing walls provides the structures with a box-like structural behavior, prevents external façades from falling over during earthquakes, and increases earthquake performance. It has been observed in the region that horizontal diaphragms prevented the out-of-plane falling mechanism of the



Fig. 26 Examples of tensile cracks at joints in arches, vaults, and domes, out-of-plane movements



Fig. 27 Examples of damage to minarets

facade walls. Moreover, the use of steel tensioners in the masonry construction technique contributed to preventing wall collapses. As a result, since most of the architectural heritage masonry buildings are still in use in the region and Türkiye, it should be noted that they are susceptible to seismic effects due to their both high specific mass and low tensile strength.

Consequently, the damage to the masonry buildings in the region occurred in the form of shear failure, opening in the joints, out-of-plane movement and overturning due to the weakness of the building elements and mortar quality, weak tension connections, weak floor diaphragms, and non-compliance with the construction rules in wall joints. In most damaged masonry structures, poor connection between structural members and wall layers, irregular structure, and weak and deteriorated materials were observed. The out-of-plane collapse of the main walls generally occurred either due to the failure of the material's compressive strength or by the wall layer's separation or slippage. Another form of damage observed after cracking is that the walls split and fell out of the plane in blocks. However, it has been observed that masonry buildings with good seismic performance in the examined region have the following characteristics: (i) A well-arranged connection between the walls or between the wall and the diaphragm provides an effective box behavior, (ii) The transverse connection between the wall layers is ensured properly, (iii) Masonry units have

a regular shape and arrangement, and (iv) The mechanical properties of the building units and the mortar are very good.

8 Conclusions

This study has comprehensively assessed the geotechnical and structural aspects following the 2023 Kahramanmaraş earthquakes. The research conducted by a team of experts has yielded valuable insights into the performance of the built environment, considering factors such as structural damage, local site conditions, and strong ground motion data. The key findings of this investigation are summarized as follows:

- The vulnerability of settlements in Antakya district of Hatay, Türkoğlu district of Kahramanmaraş, and Gölbaşı district of Adıyaman, characterized by a high incidence of demolitions and structural damages, is attributed to their locations on alluvial deposits surrounding the Amik Plain. These areas, fed by old lake beds and the Asi River, exhibit significant amplification of seismic ground motion amplitudes due to soft soil conditions. Failure to implement earthquake-resistant foundation designs for problematic soils, as recommended in geotechnical survey reports, has led to many collapsed buildings, resulting in loss of life and property. Despite their distance from the earthquake epicenter, settlements like Hatay/Kırkhan and Gaziantep/İslahiye have experienced a heightened impact on building collapses and severe damage due to their proximity to fault lines.
- The vertical component of ground motion produced by the earthquake along the Eastern Anatolian fault has been as influential as the horizontal component. That has exacerbated the soft-story problem in multi-story residential buildings with cantilevered slab floors, ultimately leading to building collapses or rendering them unusable.
- Severe damage or collapse in reinforced concrete buildings is primarily attributed to factors such as poor material quality, the soft-story effect, strong column-weak beam behavior, oversized and heavy overhangs, insufficient beam-column joints, and unconfined infill and gable walls.
- Widespread damage in precast structures was characterized by the detachment of horizontal beams from column corbels, inadequate connections leading to roof purlin collapses, and compromised structural integrity due to poor joint responses and pin connections. Architectural and structural arrangement errors introduced torsional effects, separating beams from columns, while severe damage and collapses were common in structures with weak columns and heavy roof beams. Infill wall issues were also prevalent, attributed to low-strength materials and a lack of horizontal reinforcement. Lastly, column-foundation nodes exhibited various structural problems, including bending cracks, shell concrete separation, reinforcement buckling, and damage to reinforcement integrity.
- Historical buildings in the region, constructed with shorter vibration periods on more favorable soil conditions, have experienced more extensive damage when compared to large-period reinforced concrete structures. This phenomenon is ascribed to the presence of larger horizontal and vertical spectral accelerations, which depend on the vibration period and construction techniques. Damage to masonry buildings in the area has materialized as shear failures, joint openings, out-of-plane movements, and overturning, primarily attributable to structural element weaknesses, mortar quality deficiencies, inadequately strong tension con-

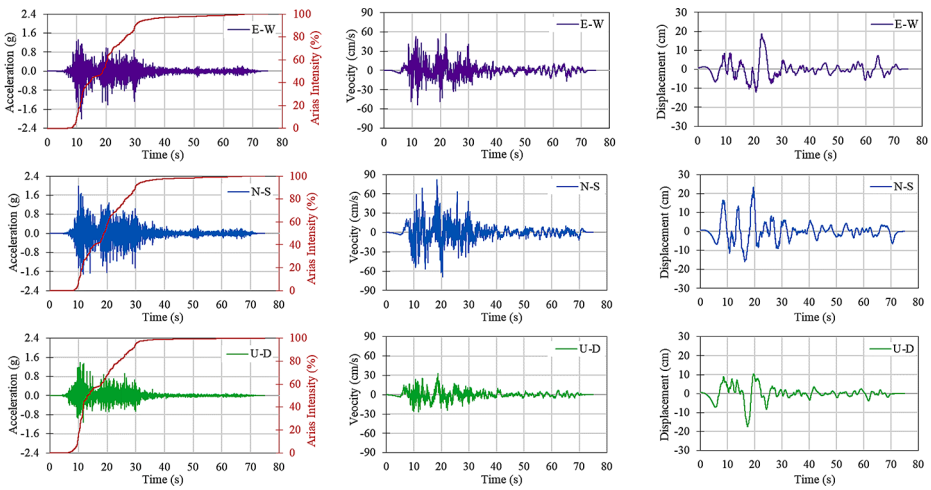


Fig. A1 Pazarcık (Kahramanmaraş) Earthquake ($M_w = 7.7$), Station 4614 (Kahramanmaraş/Pazarcık), Acceleration vs. Arias Intensity, Velocity and Displacement time histories ($V_{s,30} = 541$ m/s, Soil class: ZC)

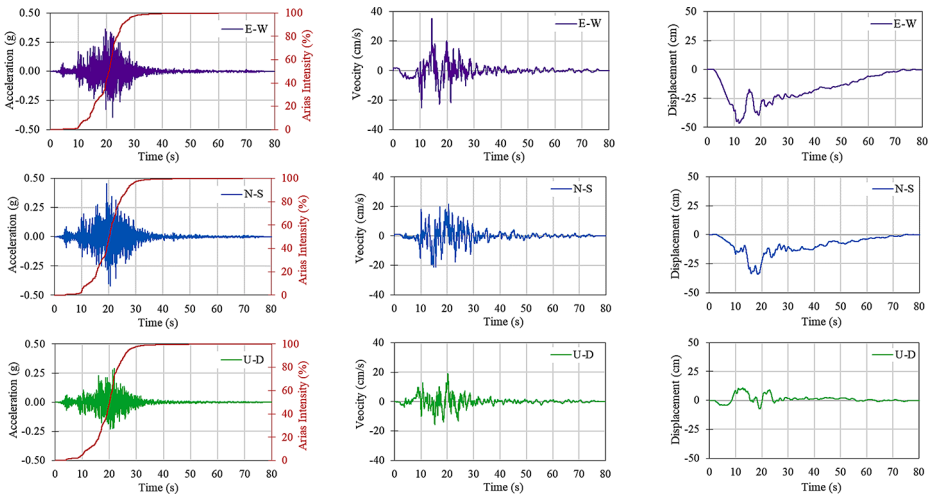


Fig. A2 Elbistan (Kahramanmaraş) Earthquake ($M_w = 7.6$), Station 4406 (Malatya/Akçadağ), Acceleration vs. Arias Intensity, Velocity and Displacement time histories ($V_{s,30} = 815$ m/s, Soil class: ZB)

nections, weak floor diaphragms, and non-compliance with construction standards in wall joints.

Appendix A

Figs. A1 and A2.

Acknowledgements The authors would like to acknowledge sincere thanks to The Scientific and Technological Research Council of Türkiye (TÜBİTAK), for supporting and funding the site investigations with 1002-C Natural Disasters - Focused Fieldwork Emergency Investigation program.

Author contributions All authors contributed to the study equally. All authors read and approved the final manuscript.

Funding Open access funding provided by the Scientific and Technological Research Council of Türkiye (TÜBİTAK). The authors would like to acknowledge The Scientific and Technological Research Council of Türkiye (TÜBİTAK), for supporting and funding the site investigations with 1002-C Natural Disasters - Focused Fieldwork Emergency Investigation program. Open access funding provided by the Scientific and Technological Research Council of Türkiye (TÜBİTAK).

Declarations

Competing Interests The authors have no relevant financial or non-financial interests to disclose.


Open Access This article is licensed under a Creative Commons Attribution 4.0 International License, which permits use, sharing, adaptation, distribution and reproduction in any medium or format, as long as you give appropriate credit to the original author(s) and the source, provide a link to the Creative Commons licence, and indicate if changes were made. The images or other third party material in this article are included in the article's Creative Commons licence, unless indicated otherwise in a credit line to the material. If material is not included in the article's Creative Commons licence and your intended use is not permitted by statutory regulation or exceeds the permitted use, you will need to obtain permission directly from the copyright holder. To view a copy of this licence, visit <http://creativecommons.org/licenses/by/4.0/>.

References

- AFAD (2023) 06 Şubat 2023 Kahramanmaraş (Pazarcık ve Elbistan) Depremleri Saha Çalışmaları Ön Değerlendirme Raporu (in Turkish), Disaster and Emergency Presidency of Türkiye. https://deprem.afad.gov.tr/assets/pdf/Arazi_Onrapor_28022023_surum1_revize.pdf. Accessed 1 November 2023
- Akıl B, Akpınar K, Üçkardeşler C, Araz H, Sağlam M, Üran ŞB (2008) Doğu Anadolu Fay Zonu Üzerinde Yer Alan Gölbaşı (Adıyaman) Yerleşim Alanındaki Zeminlerin Jeoteknik Özellikleri ve Değerlendirilmesi/ Evaluation of settlement suitability of Gölbaşı (Adıyaman) Town, located on the East Anatolian Fault Zone. *Türkiye Jeoloji Bülteni* 51(1):43–57
- Ambraseys NN (1989) Temporary seismic quiescence: SE Turkey. *Geophys J Int* 96:311–331. <https://doi.org/10.1111/j.1365-246X.1989.tb04453.x>
- Barka AA, Kadinsky-Cade K (1988) Strike-slip fault geometry in Turkey and its influence on earthquake activity. *Tectonics* 7:663–684. <https://doi.org/10.1029/TC007i003p00663>
- Barka A, Reilinger R (1997) Active tectonics of the Eastern Mediterranean region: deduced from GPS, neotectonic and seismicity data. 3
- Bulut F, Bohnhoff M, Eken T et al (2012) The East Anatolian Fault Zone: seismotectonic setting and spatio-temporal characteristics of seismicity based on precise earthquake locations. *J Geophys Res Solid Earth* 117. <https://doi.org/10.1029/2011JB008966>
- Cetin K, Ilgaç M (2023) Reconnaissance Report on February 6, 2023 Kahramanmaraş-Pazarcık (Mw=7.7) and Elbistan (Mw=7.6) Earthquakes. <https://doi.org/10.13140/RG.2.2.15569.61283/1>
- Demir A (2022) Progressive collapse resistance of low and mid-rise RC mercantile buildings subjected to a column failure. *Struct Eng Mech* 83(4):563–576. <https://doi.org/10.12989/sem.2022.83.4.563>
- Duman TY, Emre Ö (2013) The East Anatolian Fault: geometry, segmentation and jog characteristics. *Geol Soc* 372:495–529. <https://doi.org/10.1144/SP372.14>
- Emre Ö, Duman T, Özalp S et al (2013) Active Fault Map of Turkey with an Explanatory Text. 1:1,250,000 Scale
- Garini E, Gazetas G, Anastasopoulos I (2017) Evidence of significant forward rupture directivity aggravated by soil response in an M w 6 earthquake and the effects on monuments. *Earthq Eng Struct Dyn* 46:2103–2120. <https://doi.org/10.1002/eqe.2895>

- Günaydin M, Atmaca B, Demir S et al (2021) Seismic damage assessment of masonry buildings in Elazığ and Malatya following the 2020 Elazığ-Sivrice earthquake, Turkey. *Bull Earthq Eng* 19:2421–2456. <https://doi.org/10.1007/s10518-021-01073-5>
- ITU (2023) 6 Şubat 2023 04.17 Mw 7,8 Kahramanmaraş (Pazarcık, Türkoğlu), Hatay (Kırıkhan), ve 13.24 Mw 7,7 Kahramanmaraş (Elbistan/Nurhak-Çardak) Depremleri Ön İnceleme Raporu (in Turkish), Istanbul Technical University. https://haberler.itu.edu.tr/docs/default-source/default-document-library/2023_itu_deprem_on_raporu.pdf. Accessed 1 November 2023
- Karabacak V, Özkaymak Ç, Sözbilir H et al (2023) The 2023 Pazarcık (Kahramanmaraş, Türkiye) Earthquake (Mw: 7.7): implications for surface rupture dynamics along the East Anatolian Fault Zone KOERI, Earthquake Research Institute Department of Earthquake Engineering (2023) Strong Ground Motion and Building Damage Estimations Preliminary Report (v6), Boğaziçi University Kandilli Observatory and. https://eqe.bogazici.edu.tr/sites/eqe.boun.edu.tr/files/kahramanmaraş-gaziantep_earthquake_06-02-2023_04.17-bogazici_university_earthquake_engineering_department_v6.pdf. Accessed 1 November 2023
- Less T, Demir A, Sezen H (2023) Structural performance and corrosion resistance of fiber reinforced polymer wrapped steel reinforcing bars. *Constr Build Mater* 366:130176. <https://doi.org/10.1016/j.conbuildmat.2022.130176>
- McClusky S, Balassanian S, Barka A et al (2000) Global positioning system constraints on plate kinematics and dynamics in the eastern Mediterranean and Caucasus. *J Geophys Res Solid Earth* 105:5695–5719. <https://doi.org/10.1029/1999JB900351>
- McKenzie D (1972) Active tectonics of the Mediterranean Region. *Geophys J Int* 30:109–185. <https://doi.org/10.1111/j.1365-246X.1972.tb02351.x>
- Nalbant SS, McCloskey J, Steacy S, Barka AA (2002) Stress accumulation and increased seismic risk in eastern Turkey. *Earth Planet Sci Lett* 195:291–298. [https://doi.org/10.1016/S0012-821X\(01\)00592-1](https://doi.org/10.1016/S0012-821X(01)00592-1)
- Olabi MN, Caglar N, Arslan ME et al (2022) Response of nonconforming RC shear walls with smooth bars under quasi-static cyclic loading. *Bull Earthq Eng* 20:6683–6704. <https://doi.org/10.1007/s10518-022-01451-7>
- PSBD (2023) 2023 Kahramanmaraş and Hatay Earthquakes Report (in Turkish), Presidential Strategy and Budget Directorate. <https://www.sbb.gov.tr/wp-content/uploads/2023/03/2023-Kahramanmaraş-and-Hatay-Earthquakes-Report.pdf>. Accessed 1 November 2023
- Reilinger R, McClusky S, Vernant P et al (2006) GPS constraints on continental deformation in the Africa-Arabia-Eurasia continental collision zone and implications for the dynamics of plate interactions. *J Geophys Res Solid Earth* 111. <https://doi.org/10.1029/2005JB004051>
- Sagbas G, Garjan RS, Sarıkaya K, Deniz D (2023) Field reconnaissance on seismic performance and functionality of Turkish industrial facilities affected by the 2023 Kahramanmaraş earthquake sequence. *Bull Earthq Eng*. <https://doi.org/10.1007/s10518-023-01741-8>
- Şengör AMC, Yılmaz Y (1981) Tethyan evolution of Turkey: a plate tectonic approach. *Tectonophysics* 75:181–241. [https://doi.org/10.1016/0040-1951\(81\)90275-4](https://doi.org/10.1016/0040-1951(81)90275-4)
- Şengör AMC, Görür N, Şaroğlu F (1985) Strike-Slip Faulting and Related Basin Formation in Zones of Tectonic Escape: Turkey as a Case Study. In: *Strike-Slip Deformation, Basin Formation, and Sedimentation*. SEPM (Society for Sedimentary Geology) 211–226
- TADAS (2023) Turkish Accelerometric Database and Analysis System. Disaster and Emergency Presidency of Türkiye (AFAD), www.tadas.afad.gov.tr. Accessed 1 November 2023
- Tan O, Pabuççu Z, Tapırdamaz MC et al (2011) Aftershock study and seismotectonic implications of the 8 March 2010 Kovancılar (Elazığ, Turkey) earthquake (mw=6.1). *Geophys Res Lett* 38:L11304. <https://doi.org/10.1029/2011GL047702>
- Taymaz T, Eyidoğan H, Jackson J (1991) Source parameters of large earthquakes in the East Anatolian Fault Zone (Turkey). *Geophys J Int* 106:537–550. <https://doi.org/10.1111/j.1365-246X.1991.tb06328.x>
- TBEC (2018) Turkish building Earthquake Code. Turkish Ministry of Environment and Urbanization, Ankara, Türkiye
- Utkucu M, Budakoğlu E, Çabuk M (2018) Teleseismic finite-fault inversion of two mw=6.4 earthquakes along the East Anatolian Fault Zone in Turkey: the 1998 Adana and 2003 Bingöl earthquakes. *Arab J Geosci* 11:721. <https://doi.org/10.1007/s12517-018-4089-y>
- Xu J, Liu C, Xiong X (2020) Source process of the 24 January 2020 mw 6.7 East Anatolian Fault Zone, Turkey, Earthquake. *Seismol Res Lett* 91:3120–3128. <https://doi.org/10.1785/0220200124>

Authors and Affiliations

Aydin Demir¹  · **Erkan Celebi¹** · **Hakan Ozturk¹** · **Zeki Ozcan¹** · **Askin Ozocak¹** · **Ertan Bol¹** · **Sedat Sert¹** · **F. Zehra Sahin¹** · **Eylem Arslan¹** · **Zeynep Dere Yaman¹** · **Murat Utkucu²** · **Necati Mert¹**

✉ Aydin Demir
aydindemir@sakarya.edu.tr

¹ Department of Civil Engineering, Faculty of Engineering, Sakarya University, Sakarya 54050, Turkey

² Department of Geophysical Engineering, Faculty of Engineering, Sakarya University, Sakarya 54050, Turkey